Desalination and Water Treatment
www.deswater.com

doi: 10.5004/dwt.2017.20127

64 (2017) 81–89
February

Multifunctional hyperbranched polyglycerol-grafted silica-encapsulated superparamagnetic iron oxide nanoparticles as novel and reusable draw agents in forward osmosis process

Razieh Nazari[a], Marzieh Aghababaie[a], Amir Razmjou[a,*], Amir Landarani-Isfahani[b,*], Mina Amini[b], Marzieh Hajjari[b], Valiollah Mirkhani[b], Majid Moghadam[b], Asghar Taheri-Kafrani[a]

[a]*Biotechnology Department, Faculty of Advanced Sciences and Technologies, University of Isfahan, Isfahan, Iran, emails: a.razmjou@ast.ui.ac.ir (A. Razmjou), fantom.rohan@gmail.com (R. Nazari), maz_babaie@yahoo.com (M. Aghababaie), a.taheri@ast.ui.ac.ir (A. Taheri-Kafrani)*
[b]*Department of Chemistry, Catalysis Division, University of Isfahan, Isfahan, Iran, emails: landarani@Sci.ui.ac.ir (A. Landarani-Isfahani), aminimina1395@gmail.com (M. Amini), hajjarimarzieh@gmail.com (M. Hajjari), Mirkhani@sci.ui.ac.ir (V. Mirkhani), moghadamm@sci.ui.ac.ir (M. Moghadam)*

Received 7 March 2016; Accepted 4 August 2016

ABSTRACT

Forward osmosis (FO) has gained attention recently due to its low cost and energy consumption while it happens naturally. However, finding a proper draw agent for this process is a challenging task. Magnetic nanoparticles, especially with modified surfaces, have been reported as a promising draw agent, which can be easily recovered by using a magnetic field. Here, an attempt was made to study the effect of different superparamagnetic iron oxide nanoparticles (SPIONs) surface engineering on the osmotic pressure, hydrophilicity, degree of agglomeration of nanoparticles and also water flux. In this study, the osmotic potential of naked Fe_3O_4, silica-coated superparamagnetic iron oxide nanoparticles (SPION@SiO_2), hyperbranched polyglycerol/carboxylate-functionalized SPION (SPION@SiO_2@HPG and SPION@SiO_2@HPG-CO_2H) were evaluated for FO process. The effect of ionized SPIONs on the water flux has been studied for the first time, too. The SPIONs were characterized by scanning electron microscopy, transmission electron microscopy, X-ray powder diffraction, Fourier transform infrared, vibrating sample magnetometer and thermogravimetric analysis. The average of water flux in a long-term performance of FO for the introduced draw agents increased in the order of SPION < SPION@SiO_2 < SPION@SiO_2@HPG < SPION@SiO_2@HPG-CO_2H due to higher hydrophilicity and lesser agglomerations and precipitation. It was surprisingly observed that water flux of ionic magnetic draw solution behaves differently comparing with the non-ionic ones. It was revealed that ionic SPIONs at high concentration led to the formation of non-ideal polyelectrolyte solution that produces a high osmotic pressure. However, by the permeation of water, a transition from non-ideal to ideal solution at some point was observed during FO process.

Keywords: Forward osmosis; Draw agents; Ionized SPIONs; Surface engineering

* Corresponding authors.

1. Introduction

Forward osmosis (FO) is one of the promising membrane technologies that has gained a global attention due to its easy and economic use for water reuse [1–3], sea water desalination [4,5], food processing [6], protein concentration [5,7], and radioactive liquid waste treatment [8]. Generally, transport of water across a semi-permeable membrane from a lower solute concentration region to the higher one is known as osmosis [3]. In living organism, osmosis plays a vital role in keeping cells normal cytosolic osmolality and also adjusting the cell volume through swelling or shrinking in hypotonic or hypertonic solutions, respectively [9]. Thus, the principles of direct osmosis in biological membrane phenomenon have been utilized in FO desalination. FO process needs both semi-permeable membrane and an osmotic pressure difference (OPD) across the membrane, which can be induced by draw agent or draw solution (DS) [10]. However, the search for new DSs has become the Holy Grail of FO and has presented new draw agents with a few criteria such as availability, low cost, non-toxicity (particularly for potable water production), easily regeneration, no reverse flux, and compatibility with membrane surface [10–12]. According to Ge et al. [10] the studied draw agents can be categorized into commercially available (volatile and nutrient compounds, inorganic and organic salts, and polymers) and synthetic (hydrogels, hybrid materials, magnetic nanoparticles [MNPs], etc.) compounds. A typical FO membrane process has two main stages of membrane process (water desalination, protein enrichment, etc.) and draw agent recovery [11]. In the first stage, the draw agent induces osmotic pressure gradient across the membrane to drive water molecules from feed to permeate membrane side. In the second stage, the draw agent needs to be recovered from the permeate water to continue the process [13]. Therefore, one of the main obstacles for commercial implementation of FO is a need for the full recovery of draw agents at a low energy cost without compromising their high osmotic pressure [14]. Another important characteristic of draw agents is their response to external stimuli such as pressure, temperature, light, and magnetic field [3].

Recently, MNPs have been considered as new draw agents in FO process due to their excellent properties such as: superparamagnetism, high surface area to volume ratio, low toxicity, biocompatibility, easy separation, and their compatibility to functionalization [15]. The first attempt to investigate engineered MNPs as draw solutes in FO process was conducted by Liu et al. [16]. They reported that MNPs with high molecular weight and low solubility could not provide a high osmotic pressure. However, it was found that the smaller and less viscous MNPs with a greater hydrophilic surface area (such as poly(ethelene glycol)-coated [PEG-coated] MNPs) had a significantly higher osmotic pressure [16]. Then, Ling et al. [1] used hydrophilic MNPs with three different surface functional groups (2-pyrrolidone, triethylene glycol, and polyacrylic acid) to increase hydrophilicity and water flux [1]. They investigated the possible factors that could affect the performance of MNPs as draw solute in FO and pressure-retarded osmosis (PRO) systems and showed that the particle size distribution and concentration of draw agents are the important ones. According to their researches, water flux can be enhanced by decreasing the diameters of MNPs [1]. The hydrophilic polyacrylic-coated MNPs of 6 nm in diameter were examined for desalination in Forward Osmosis-Ultrafiltration process (FO-UF process) and showed a higher water flux than the uncoated MNPs [1,7]. Bai et al. [17] introduced the dextran-coated Fe_3O_4 MNPs as a new draw solute for brackish water desalination and showed an average water flux of almost 9 LMH [17]. In the same year, Ge et al. [18] synthesized PEG-$(CO_2H)_2$-coated MNPs with different size distributions (from 4.2 to 17.5 nm) and investigated their performance in FO and PRO process. They also reported that the size and concentration of nanoparticles play important roles in water permeation flux and its quality. The water permeation flux increased with increasing the DS concentration. In this way, according to the size and concentration, water flux of >4 LMH were attained [18]. Recently, carboxylated polyglycerol-coated MNPs were synthesized as draw agents for radioactive liquid waste treatment by Yang et al. [8], too. These MNPs showed a good colloidal stability in aqueous solution and enough high osmolality and osmotic pressure to be used as a draw solute in FO process [8]. Then, Na et al. [15] used superhydrophilic citrate-coated MNP (Cit-MNP) as draw solute, which provided a high initial water flux of 17.3 LMH.

Magnetic poly(N-isopropylacrylamide-co-sodium-2-acrylamido-2-methylpropane sulfonate, Fe_3O_4@P [NIPAM-co-AMPS]) nanogels with a core diameter of 10–20 nm were prepared by Zhou et al. [19]. These thermoresponsive ionic nanogels produced water flux of about 0.26 LMH, which were 2.5 times higher than magnetic weak ionic nanogels of Fe_3O_4@P (NIPAM-co-acrylic acid) under the same operating conditions [19].

Despite a lot of researches in this area, there is an inconsistency in the reported water fluxes using magnetic DSs such as a broad range of fluxes (17.3 LMH [15], 9 LMH [17], 4 LMH [18], 0.26 LMH [19]) using similar membrane (mostly from Hydration Technologies Inc., USA). This inconsistency has been attributed to the size, molecular weight, concentration, agglomeration, and terminal groups of the MNPs. The chemical potential of the feed solution and therefore OPD is the main issue on which all of the above-mentioned factors could have a considerable effect. In this regard, developing an FO magnetic draw agent with high osmotic pressure, minimal reverse flux, low viscosity, low molecular weight, low agglomeration tendency, smaller size and good compatibility with membrane is still a controversial challenge [20]. The agglomeration of MNPs has been guessed as the most critical issues and source of inconstancy in the results during FO and draw agent recovering process. To address the issue, surface engineering of magnetic draw solutes has been recommended to improve the performance of MNPs as draw agent. The effect of introducing ionic terminal groups onto the surface of MNPs has not been investigated on the FO performance.

In this study, superparamagnetic iron oxide nanoparticles (SPIONs) hybrids were synthesized using co-precipitation method and functionalized with different materials to increase their hydrophilicity and osmotic pressure as well as to reduce agglomeration tendency. In addition, having SPIONs without functionalization leads to sever agglomerations and may cause the partial precipitation of particles and change in hydrodynamic sizes. Here, the functionalization of the nanoparticles will avoid particle concentration and size variations during FO process. In this way, SPIONs,

silica-coated superparamagnetic iron oxide nanoparticles (SPION@SiO_2), hyperbranched polyglycerol (HPG) grafted SPION@SiO_2 (SPION@SiO_2@HPG) and carboxylic groups derived from HPG SPION@SiO_2@HPG (SPION@SiO_2@HPG-CO_2H) were tested in a lab-scale FO system during 5 d to study the effect of SPIONs surface modification on the FO performance.

Afterward, SPION@SiO_2@HPG and SPION@SiO_2@HPG-CO_2H were ionized with $–O^-Na^+$ and $–CO_2^-Na^+$ terminal groups and introduced as novel DSs for FO process for the first time. These ionized SPIONs release Na^+ ions into the permeate solution and boost the osmotic pressure. It was also attempted, for the first time, to understand the effect of ionization of the presented SPIONs on the FO performance as well. In fact, the focus of this work was on increasing the water flux by improving the OPD and increasing the solubility and dispersibility of SPIONs using surface modification and reducing agglomeration tendency of SPIONs.

2. Material and methods

2.1. Materials

The iron (II) chloride tetrahydrate ($FeCl_2{\cdot}4H_2O$, 99.7%), iron (III) chloride hexahydrate ($FeCl_3{\cdot}6H_2O$, 99.0%), tetraethyl orthosilicate (TEOS, 28%), ammonia ($NH_3{\cdot}H_2O$, 25 wt%), ethanol (C_2H_5OH,99.7%), *N,N*-dimethylformamide ($HCON(CH_3)_2$, ≥99.5%), succinic anhydride ($C_4H_4O_3$, ≥98.0%(m)) and triethylamine (($(C_2H_5)_3N$, ≥99.0% (a/a)), sodium methoxide (NaOMe ≥97%(m)) and NaCl were supplied by Merck. Methanol (CH_3OH, 99.96%) were purchased from Samchun Pure Chemical Co., Korea. The deionized (DI) water used in all experiments was also produced with a Milli-Q unit (Merck Millipore).

2.2. MNPs synthesis

2.2.1. Synthesis of SPIONs

The SPIONs were made by co-precipitation method [21,22]. An aqueous solution of $FeCl_3$ and $FeCl_2$ were mixed at a ratio of 2:1 in 200 ml DI water and stirred vigorously with a mechanical stirrer under a nitrogen atmosphere at 60°C. After 15 min, 6 mL of 25% ammonia was added into the solution with vigorous stirring for 30–40 min to raise the pH to 9. The black precipitate was washed several times with DI water and ethanol and freeze dried in vacuum.

Silica-encapsulated SPIONs (SPION@SiO_2) were prepared through sol–gel process [22]. Obtained magnetite nanoparticles were redispersed in 200 ml ethanol by vigorous stirring and sonicated in the presence of nitrogen gas. Then, 30 ml of DI water and 15 ml of NH_4OH were added to the solution. TEOS (2 ml) was added to the homogenized mixture and stirred for 5 h. Afterward, the SPION@SiO_2 were washed with ethanol and water and dried at room temperature.

2.2.2. Preparation of SPION@SiO_2@HPG-CO_2H and SPION@SiO_2@HPG-CO_2H

Hyperbranched polyglycerol functionalized SPION@SiO_2 (SPION@SiO_2@HPG) was prepared according to the literature [23,24]. Typically, in a glove box containing nitrogen atmosphere, a mixture of SPION (100 mg) and sodium methoxide (50 mg) in methanol (1 mL) was sonicated by an ultrasonic bath for 30 min. Next, the SPIONs were separated by external magnetic and washed by dried ethanol. Then, 20 mL of anhydrous dioxane was added to desired nanoparticles, and the flask was kept in an oil bath at 100°C. Glycidol (2 ml) was added dropwise to the above mixture. Then, it was cooled, and the contents were dissolved in methanol. Subsequently, the product was separated by a magnet and washed with methanol under sonication. The resulting nanoparticles were dried in a vacuum to give the SPION@SiO_2@HPG.

To prepare SPION@SiO_2@HPG-CO_2H hybrids, typically, a mixture of SPION@SiO_2@HPG (100 mg) and *N,N*-dimethyl formamide (10 ml) were exposed to ultrasonic waves for 10 min. Then, succinic anhydride (80 mg) and triethylamine (15 ml) were added to the mixture and then sonicated for 10 min. After that, the mixture was stirred at 60°C for 4 h. The resulting sample (designed as SPION@SiO_2@HPG-CO_2H) was separated using a magnet and washed with methanol several times.

The preparation processes of SPION@SiO_2@HPG and SPION@SiO_2@HPG-CO_2H were shown in Fig. 1.

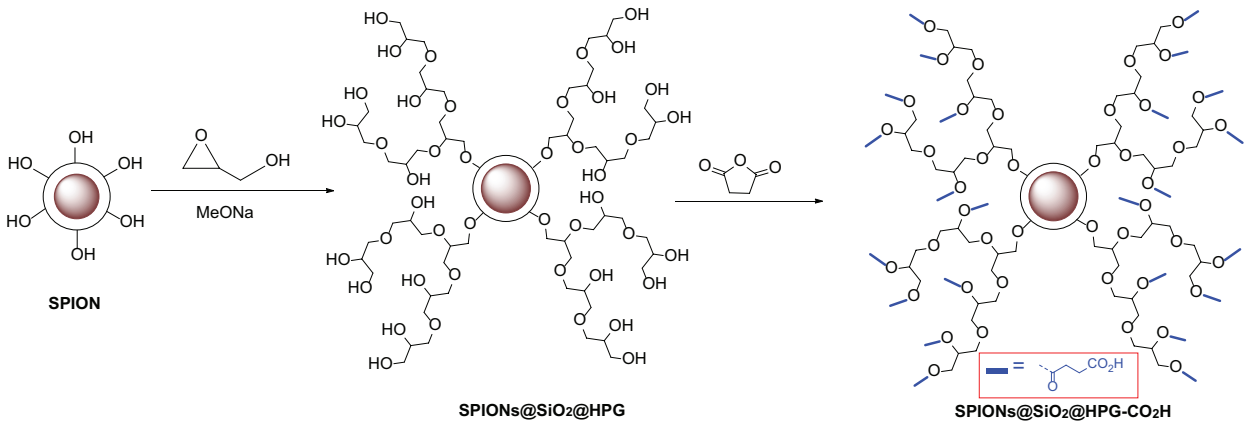

Fig. 1. Preparation route for SPION@SiO_2@HPG-CO_2H.

2.2.3. Ionic SPION@SiO_2@HPG and SPION@SiO_2@HPG-CO_2H

The SPION@SiO_2@HPG and SPION@SiO_2@HPG-CO_2H can be easily changed to salt formats ($–O^-Na^+$ and $–CO_2^-Na^+$, respectively) using sodium methoxide as base. In this way, 5 mg of nanoparticles (SPION@SiO_2@HPG or SPION@SiO_2@HPG-CO_2H) were dispersed in absolute methanol. Next, 3 mg sodium methoxide were added to each solution and dispersed and sonicated in an ultrasonic bath for 15 min. Then, the SPIONs were separated using an external magnet, washed three times with dry methanol and dried in a vacuum oven at 60°C.

2.3. FO process

As shown in Fig. 2, the performance of the prepared SPIONs were tested in a lab-scale FO system as the DSs. A cellulose triacetate flat-sheet FO cartridge membrane (4.52 cm^2) with an embedded polyester screen mesh from Hydration Technologies Inc. was used. 5 mg of each SPIONs were dispersed in 1 ml of Milli-Q water (5 g/l), for 20 min, using an ultrasonic system. The water flux (J, $L.m^{-2}.h^{-1}$) was calculated from the following equation:

$$J = \Delta W / \left(A.\Delta t\right) \quad (1)$$

where ΔW (kg) was the weight of permeation water; Δt (h) was time; and A (m^2) was the area of used membrane. It should be noted that to exclude the effect of internal concentration polarization (ICP) and also fouling on the flux decline, the DI water was considered as the feed solution. In this way, it was exclusively possible to study the effect of nanoparticles characteristic such as dispersion quality, agglomeration, and surface charge on the FO performance.

2.4. Characterization

2.4.1. Scanning and transmission electron microscopy (SEM and TEM)

To study the SPIONs structure and particle size, a field emission scanning electron microscopy (FESEM; Hitachi S-4160) and a field emission transmission electron microscopy (FETEM; Philips CM30, operating at 200 kV) were used. These measurements were made by the sonication of the SPIONs in ethanol for several minutes. Then, one drop of the finely divided suspension was placed on a specially produced structure less carbon support film having a thickness of 4–6 nm.

2.4.2. Fourier transform infrared spectra

Surface bonding and functional groupings of the nanoparticles were recorded by Fourier transform infrared (FTIR) spectroscopy using a FTIR spectrometer (JASCO FT/IR-6300, Japan).

2.4.3. Thermogravimetric analysis (TGA)

The amount of organic moieties in the HPG-functionalized SPIONs (SPION@SiO_2@HPG) was determined by TGA. TGA were carried out on a Mettler TG50 instrument under airflow at a uniform heating rate of 5°C/min in the range of 25°C–600°C (a Mettler TG50 model).

2.4.4. X-ray powder diffraction (XRD)

XRD spectra was taken on a Bruker D8-advance x-ray diffractometer with Cu Kα radiation to study the degree of structural order of SPIONs.

2.4.5. Vibrating sample magnetometer (VSM)

The magnetic properties of SPIONs were recorded by an alternating gradient force magnetometer, Meghnatis Daghigh Kavir Co., Iran.

3. Result and discussion

3.1. SPIONs characterization

3.1.1. SPIONs particle size

The nanostructures and morphology of SPION@SiO_2@HPG-CO_2H was studied by TEM and SEM (Fig. 3). As can be seen in the TEM image, the dark regions or black spots

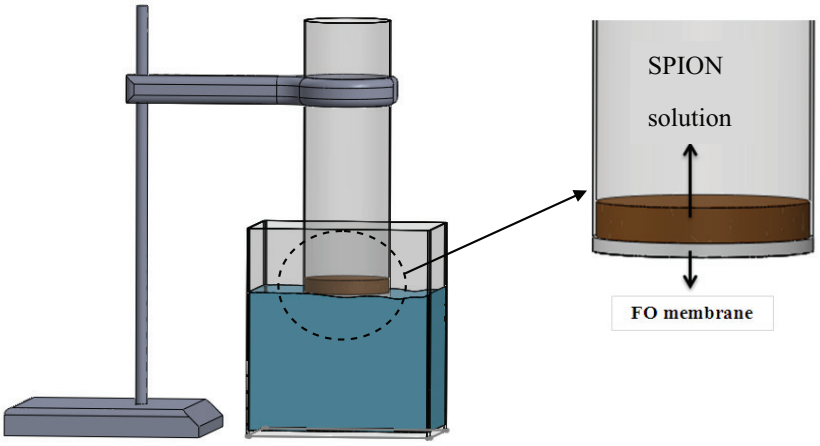

Fig. 2. A schematic of FO process.

are the SPIONs while the colorless parts belong to silica and hyperbrached polymer; this is due to the higher electron density of iron compared with other phases. Besides, the SPIONs were relatively monodisperse with the average size of 10–15 nm in diameter. A representative SEM image of SPION@SiO_2@HPG-CO_2H is shown in Fig. 3(b). The SPIONs are totally surrounded by SiO_2 and organic phase; no single SPIONs phase can be observed, which is in agreement with the TEM studies.

3.1.2. FTIR analysis of SPIONs

The FTIR spectra confirmed the coating of silica on MNPs (Figs. 4(a) and (b)). It showed that all of the four spectra had the adsorption peak corresponding to the characteristic absorption of Fe–O bond at 585 cm^{-1}. After being coated with silica, the characteristic absorption peaks corresponding to the asymmetric and symmetric stretching vibration of Si–O–Si bond in oxygen–silica tetrahedron can be clearly observed at 1,101 and 811 cm^{-1} (as Figs. 4(b)–(d)). After the polymerization, the presence of bands at 2,875 and 2,917 cm^{-1}, associated with C–H stretching and the adsorption peak of hydroxyl group (O–H) at 3,435 cm^{-1} had also increased to some extent, both of which confirms the synthesis of SPION@SiO_2@HPG (Fig. 4(c)). Finally, the terminal hydroxyl groups of HPG were transformed into carboxyl groups through the ring opening of succinic anhydride. As shown in Fig. 4(d), a new characteristic absorption peak corresponding to the stretching vibration of carbonyl groups (C=O) can be observed clearly at 1,737 cm^{-1}, which indicates that the terminal hydroxyl groups had been successfully transformed into carboxyl groups, and SPION@SiO_2@HPG-CO_2H had been successfully obtained.

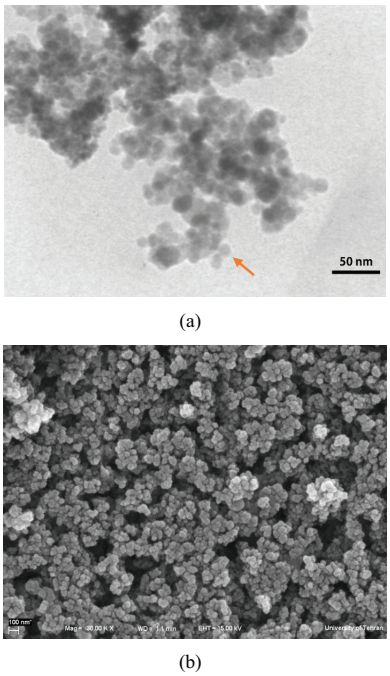

Fig. 3. (a) TEM and (b) SEM image of SPION@SiO_2@HPG-CO_2H.

3.1.3. Thermogravimetric analysis of SPIONs

The amount of organic moieties in the hydrophilic SPIONs was also determined by TGA. The weight loss of the SPION@SiO_2@HPG between 25°C and 600°C as a function of temperature was determined using TGA, which is an irreversible process because of thermal decomposition. The TGA plots of SPION, SPION@SiO_2@HPG and SPION@SiO_2@HPG-CO_2H (Fig. 5) showed a two-step thermal decomposition. The first step of weight loss (between 25°C and 200°C) in the case of SPIONs corresponds to the removal of physically adsorbed solvents, whereas, in the other cases, the main weight loss in the second step (between 200°C and 500°C) was due to the removal of organic moieties on the surface. Compared with Fig. 5(a), both of SPION@SiO_2@HPG and SPION@SiO_2@HPG-CO_2H had obvious weight loss within the range of 200°C–550°C, and the latter (~25.28%) was more than the former (~15.93%) (as Figs. 5(b) and (c)), which demonstrated that the HPG grafting and the carboxyl modification had been successfully achieved.

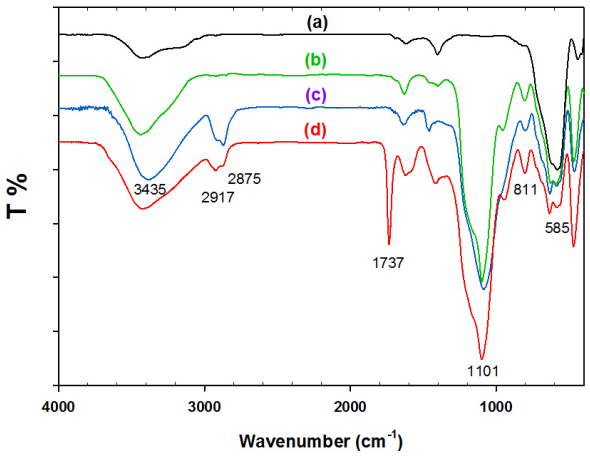

Fig. 4. The FT-IR spectra of: a) SPION, b) SPION@SiO_2, c) SPION@SiO_2@HPG and d) SPION@SiO_2@HPG-CO_2H.

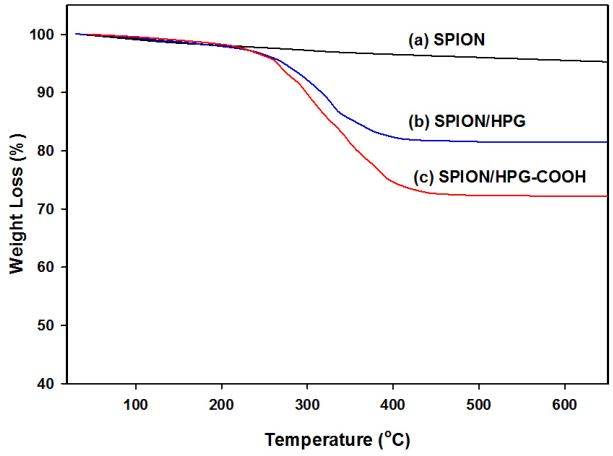

Fig. 5. TGA spectra of: a) SPION@SiO_2, b) SPION@SiO_2@HPG and c) SPION@SiO_2@HPG-CO_2H.

3.1.4. Crystallographic analysis of SPIONs

As shown in Fig. 6, a broad peak around 2θ of 2°–30° corresponding to amorphous phase of SiO_2, and the characteristic diffraction peaks at 2θ = 30.09, 35.44, 43.07, 54.43, 57.16, and 63.55 were in agreement with face-centered cubic of Fe_3O_4.

3.1.5. Magnetic properties of SPIONs

According to Fig. 7, the saturation magnetization values for SPION@SiO_2, SPION@SiO_2@HPG, and SPION@SiO_2@HPG-CO_2H were 63.1, 32.8, and 18.1 emu/g, respectively. These results showed that the saturation magnetization of SPIONs decreased with the increase of polymer shell. While MNPs were composed of two parts included a magnetic core and the polymer shell that surrounds the magnetic core, polymer shell protects magnetic core from aggregation and enables surface modification. This decrease of magnetization may also be due to polymer shell, which acts as the magnet adsorbent [15,18,25]. Nevertheless, from the figure, reducing the saturation magnetization, the nanoparticles could still be easily separated from solution by external magnet and immediately redispersed after removing the magnetic field.

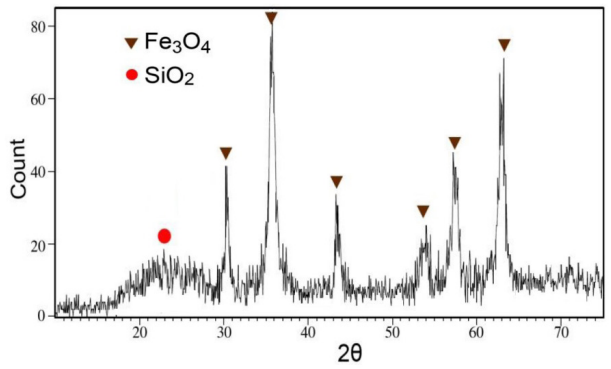

Fig. 6. XRD pattern of hydrophilic SPIONs.

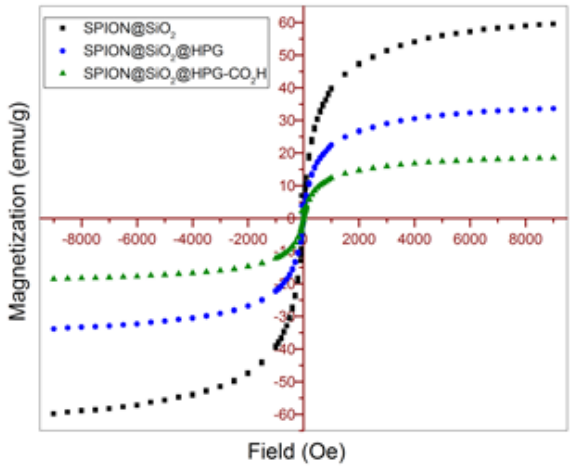

Fig. 7. Magnetization curves of different types of SPIONs.

3.2. FO performance

3.2.1. FO performance with non-ionic SPIONs

As mentioned before, water flux is related to the osmotic pressure as the main driving force in FO process and can be described by the following equation [10]:

$$J = A\sigma\Delta\pi \quad (2)$$

where A is the water permeability coefficient; σ is reflection coefficient; and Δπ is the OPD between the bulk of draw agent and feed solutions. In addition, osmotic pressure can be expressed as follow [10]:

$$\pi = iMRT = i(n'/V)RT = i(m/(wV))RT \quad (3)$$

where i is the van't Hoff factor; M is the solute molarity; R is the universal gas constant; T is the absolute temperature; n' is the number of solute moles; m is the mass of solute; w is the molecular weight of the solute; and V is the solution volume. The reduction in water flux in FO process was mainly due to the significant reduction in driving force. As time went on, water molecules traveled from feed side to the permeate side leading to an increase in the volume of the permeate (V). Based on Eq. 3, the larger the value of V, the lower the molarity of the SPIONs (M), considering the fact that n' remains constant. This led to the reduction of osmotic pressure in the solute side and water flux.

Fig. 8 shows the water flux ($L.m^{-2}.h^{-1}$) in a FO process using different DSs. As can be seen in Fig. 8(a), initially, the water flux of SPIONs was more than that of others. This higher initial flux might be due to smaller size and lower molecular weight of these SPIONs. However, it reduced sharply to the point of nearly zero, which could be due to the agglomeration as a result of their high surface energy and reduction of osmotic driving force [26]. The agglomeration of SPIONs would increase their hydrodynamic diameter, and thus, the particles were not small enough for Brownian motion to overcome gravity and particle settling [27]. This result has been observed in previous studies, which has considered the effect of size on water flux [1].

According to Fig. 8(a), by surface engineering of SPIONs, their absorption ability retained after 5 d of operation compared with SPIONs. Due to the presence of OH groups on the surface of silica-coated nanoparticle, the hydrophilic properties increased, and initial water flux of 0.143 $L.m^{-2}.h^{-1}$ was achieved. As can be seen in Fig. 8(b), the final flux of SPION@SiO_2@HPG and SPION@SiO_2@HPG-CO_2H were significantly higher than that of the other samples. It should be noted that by increasing the size and molecular weight of the SPIONs, initial water flux has decreased. However, water flux for SPION@SiO_2@HPG and SPION@SiO_2@HPG-CO_2H remained almost constant, which could be due to the higher solubility and lower agglomeration tendency of these SPIONs. Therefore, the higher flux of SPION@SiO_2, SPION@SiO_2@HPG and SPION@SiO_2@HPG-CO_2H could be due to the appearance of hydrophilic groups and its lower tendency to agglomerate. However, according to Eq. 3, all the fluxes were reduced by the permeation of water to the permeate side, which reduced the value of M and consequently

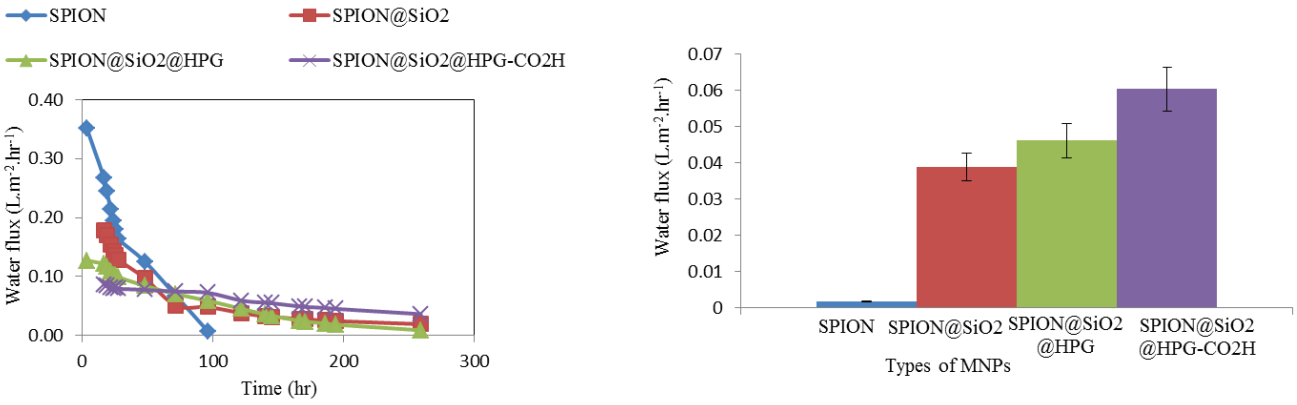

Fig. 8. Water flux of FO process (a) over 10 d and (b) at 5 d using different SPIONs as draw solution.

osmotic pressure. In addition, SPIONs settling on the membrane surface could reduce the value of *M* and driving force [11,14] and also could plug the membrane pores. The physical blocking of the membrane pores by nanoparticles was also reported elsewhere [15].

3.2.2. FO performance of ionic SPIONs

Another way to increase the osmotic pressure of the nanoparticles is to boost the van't Hoff factor. This factor is higher than 1.0 for ionic compounds, which can dissociate in solutions [28]. The effect of introducing charge to a non-ionic non-magnetic draw agent on the water flux was investigated by Li et al. [29]. They found that ionic polymer hydrogels with thermal responsive units could induce a significantly higher water permeation rates than that of non-ionic hydrogel from 0.36 to 0.30 LMH for two non-ionic hydrogels: poly(acrylamide) (PAM) and poly(*N*-isopropylacrylamid) (PNIPAM) to 0.96 and 0.55 LMH for two ionic polymer hydrogels: poly(sodium acrylate) (PSA) and poly((sodium acrylate)-co-poly(*N*-isopropylacrylamide) (PSA-NIPAM)), respectively.

In this study, ionized SPIONs were synthesized by introducing Na^+ to the SPION@SiO_2@HPG and SPION@SiO_2@HPG-CO_2H to increase van't Hoff factor following the reactions provided in Fig. 9.

As can be seen in Fig. 10, in the first 24 h, higher fluxes were observed and compared with the non-ionic SPIONs. Maximum LMH in the first 24 h for SPION@SiO_2@HPG and SPION@SiO_2@HPG-CO_2H were 0.12 and 0.085, respectively. However, the ionic form of the SPIONs resulted in a significant increase in the maximum LMH during the first 24 h, which were 0.32 and 0.43, respectively. At the end of 24 h, the total LMH of ionic SPION@SiO_2@HPG and SPION@SiO_2@HPG-CO_2H were higher than that of non-ionic ones as draw agents. It was shown that functionalizing the SPIONs with ionic and hydrophilic terminal groups increases the water flux due to the increase of osmotic pressure by highly dissociation of Na^+ ion in the solution [20].

However, according to Fig. 10, contrary to non-ionic nanoparticles, water flux has increased for the first 12 h and then decreased. This phenomenon has not been observed for the non-ionic SPIONs. While polyelectrolytes don't obey the ideal solution laws, Eq. 3 cannot be used for these ionic compounds. Generally, the theoretical osmotic pressure is a function of water activates of the solution [28,30]:

$$\Pi = (R.T / V).\ln(a) \tag{4}$$

In sufficiently dilute solutions, Eq. 3 will be applied while in the case of concentrated solutions (higher molality) Eq. 4 is used. In this case, water activity could be calculated by the following equation [31,32]:

$$a = n / (n + i.n') \tag{5}$$

where n is the number of moles of solvent; n' is the number solutes; and i is the van't Hoff factor. At the first hours of the process, solute moles (n') were high whereas water moles (n) were low. Besides, the prepared ionized SPIONS had a significantly high van't Hoff factor, which caused the second term of the denominator ($i.n'$) to be much bigger than the first term (n). Therefore, Eq. 5 could be written as follows:

$$a = n / i.n' \tag{6}$$

As a result, at the beginning of the FO process, the permeation of water leaded to the increase in water activity (a) and thus enhancing the osmotic pressure and water flux (based on Eq. 4). This flux enhancement was continued until it reached a peak point where the DS was diluted to the level of an ideal solution. From that point on, Eq. 3 was more practical, and thus, water flux was declined by the increase of volume of the solution in the draw agent side.

Another possible reason for initial flux increase in Fig. 10 could be the effect of agglomeration on ionic dissociation of SPIONs. At the beginning of the FO process, the DS was too concentrated and SPIONs were agglomerated, which forced SPIONs molecules close together with limited molecular movements. Therefore, the repulsive forces were not strong enough to fully dissociate the ionic SPIONs and overcome partial agglomerations. However, when FO process proceeded, the volume of the permeate solution increased and resulted in a higher degree of dissociation of ionic SPIONs.

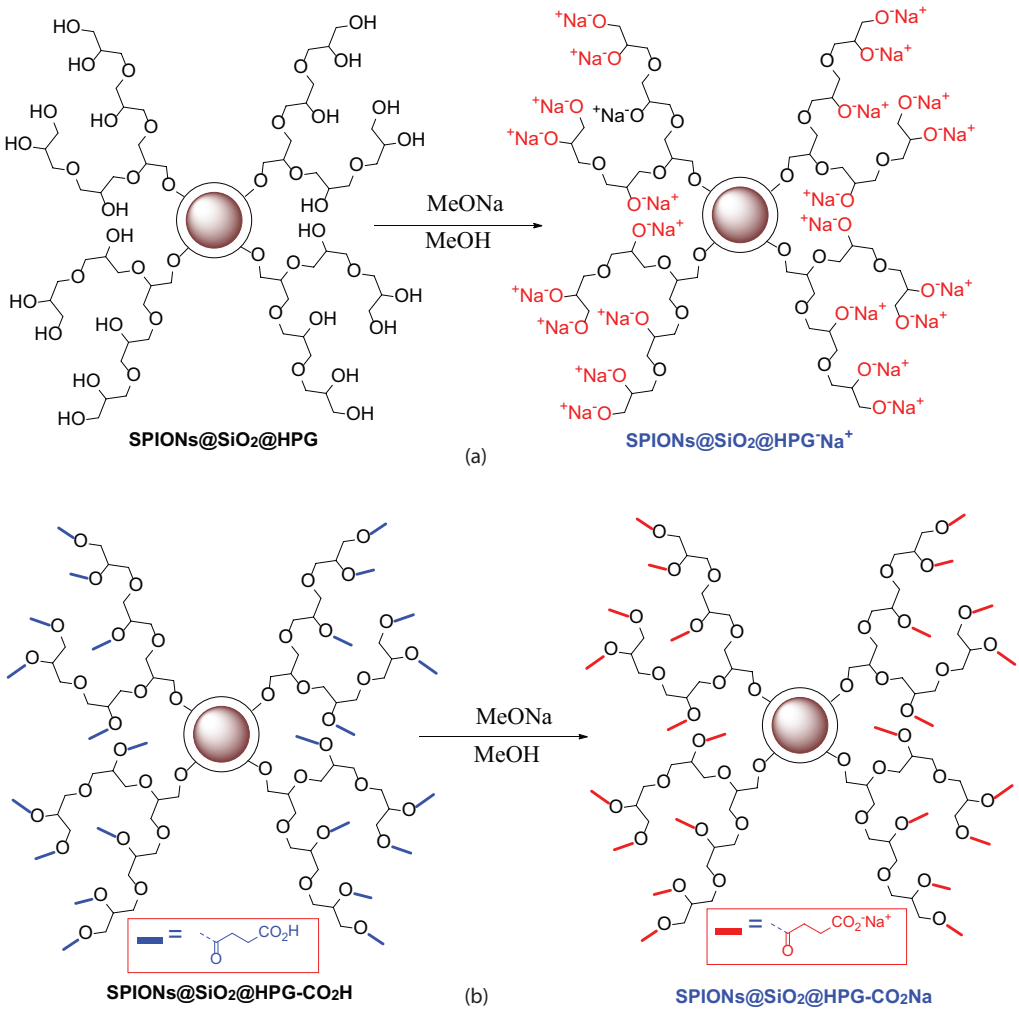

Fig. 9. Preparation of (a) Ionic SPION@SiO_2@HPG and (b) Ionic SPION@SiO_2@HPG-CO_2H.

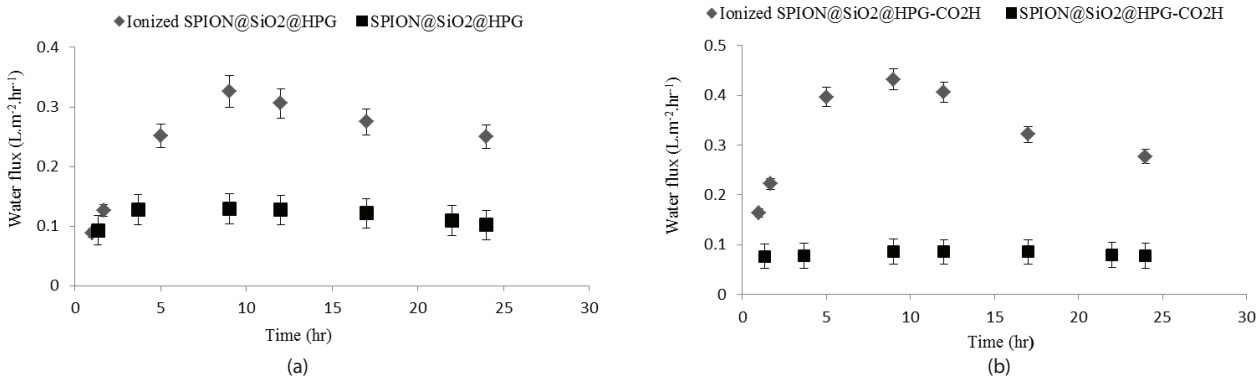

Fig. 10. Water flux vs. time for ionic and non-ionic of (a) SPION@SiO_2@HPG and (b) SPION@SiO_2@HPG-CO_2H.

The higher the degree of ionic dissociation was, the higher the van't Hoff factor and water flux were. This gradual ionic dissociation continued until it reaches its chemical equilibrium or maximum dissociation capacity. From that point on, the further increase in permeate volume resulted in the reduction of osmotic pressure and thus water flux.

4. Conclusion

In the present work, superparamagnetic iron oxide MNPs were synthesized with different coatings and functional groups and were considered as FO draw solute. It has been observed that the surface engineering of SPIONs

has increased the water flux in FO process by the addition of more hydrophilic groups. Osmotic pressure, the main driving force in the FO process, is contributed to the concentration, molecular weight and van't Hoff factor of the draw agent. It was reported that the size and solubility and agglomeration tendency of the nanoparticles are also important affecting parameters on the water flux. It has been observed that SPION@SiO_2@HPG and SPION@SiO_2@HPG-CO_2H are more suitable candidates among other reported SPIONs to be used in continuous applications as their osmotic potential remained relatively more constant due to their lower agglomeration tendency. Furthermore, functionalizing SPION@SiO_2@HPG and SPION@SiO_2@HPG-CO_2H with $–O^-Na^+$ and $–CO_2^-Na^+$ terminal groups increased the LMH by enhancing the osmotic pressure originated from the dissociation of ions and increasing the van't Hoff factor. Thus, the ionized SPIONs draw agents have the attractive properties that could introduce them as a beneficial and exclusive draw agent in FO process due to: (i) superparamagnetism property that allows magnetic (and facile) separation of SPIONs from the pure water, (ii) the new ionic structure that makes the ionic SPIONs to produce more driving force and thus more water flux, (iii) reduce agglomeration tendency due to Na^+ ions. These SPIONs has better performance as draw agents in FO process. Therefore, these nanoparticles are more appropriate to use in FO process.

Acknowledgment

The authors acknowledged the financial support of this work provided by Isfahan university research council.

References

[1] M.M. Ling, K.Y. Wang, T.S. Chung, Highly water-soluble magnetic nanoparticles as novel draw solutes in forward osmosis for water reuse, Ind. Eng. Chem. Res., 49 (2010) 5869–5876.
[2] T.S. Chung, S. Zhang, K.Y. Wang, J. Su, M.M. Ling, Forward osmosis processes: yesterday, today and tomorrow, Desalination, 287 (2012) 78–81.
[3] D. Li, H. Wang, Smart draw agents for emerging forward osmosis application, J. Mater. Chem. A., 1 (2013) 14049–14060.
[4] A. Razmjou, G. Simon, H. Wang, Polymer Hydrogels as Smart Draw Agents in Forward Osmosis Processes, Forward Osmosis: Fundamentals and Applications, American Society of Civil Engineers (ASCE), USA, 2015, pp. 129–149.
[5] M.M. Ling, T.S. Chung, Desalination process using super hydrophilic nanoparticles via forward osmosis integrated with ultrafiltration regeneration, Desalination, 278 (2011) 194–202.
[6] K.B. Petrotos, P.C. Quantick, H. Petropakis, Direct osmotic concentration of tomato juice in tubular membrane – module configuration. II. The effect of using clarified tomato juice on the process performance, J. Membr. Sci., 160 (1999) 171–177.
[7] M.M. Ling, T.S. Chung, Novel dual-stage FO system for sustainable protein enrichment using nanoparticles as intermediate draw solutes, J. Membr. Sci., 372 (2011) 201–209.
[8] H.M. Yang, K.W. Lee, J.K. Moon, Synthesis of Magnetic Nanoparticles as a Draw Solute in Forward Osmosis Membrane Process for the Treatment of Radioactive Liquid Waste, Transactions of the Korean Nuclear Society Spring Meeting, Gwangju, 2013.
[9] H. Lodish, A. Berk, S.L. Zipursky, P. Matsudaira, D. Baltimore, J. Darnell, Molecular Cell Biology, 4th ed., Scientific American Books, New York, 2000.
[10] Q. Ge, M. Ling, T.S. Chung, Draw solutions for forward osmosis processes: developments, challenges, and prospects for the future, J. Membr. Sci., 442 (2013) 225–237.
[11] A. Razmjou, G.P. Simon, H. Wang, Effect of particle size on the performance of forward osmosis desalination by stimuli-responsive polymer hydrogels as a draw agent, Chem. Eng. J., 215 (2013) 913–920.
[12] B. Van der Bruggen, P. Luis, Forward osmosis: understanding the hype, Rev. Chem. Eng., 31 (2015) 1–12.
[13] A. Razmjou, M.R. Barati, G.P. Simon, K. Suzuki, H. Wang, Fast deswelling of nanocomposite polymer hydrogels via magnetic field-induced heating for emerging FO desalination, Environ. Sci. Technol., 47 (2013) 6297–6305.
[14] L. Chekli, S. Phuntsho, H.K. Shon, S. Vigneswaran, J. Kandasamy, A. Chanan, A review of draw solutes in forward osmosis process and their use in modern applications, Desal. Wat. Treat., 43 (2012) 167–184.
[15] Y. Na, S. Yang, S. Lee, Evaluation of citrate-coated magnetic nanoparticles as draw solute for forward osmosis, Desalination, 347 (2014) 34–42.
[16] L. Liu, S. Adham, J. Oppenheimer, M. Kumar, Dewatering Reverse Osmosis Concentrate Using Forward Osmosis, Proc. Membrane Technology Conference & Exposition, 2007.
[17] H. Bai, L. Zhaoyang, D.D. Sun, Highly water soluble and recovered dextran coated Fe_3O_4 magnetic nanoparticles for brackish water desalination, Sep. Purif. Technol., 81 (2011) 392–399.
[18] Q. Ge, J. Su, T.S. Chung, G. Amy, Hydrophilic superparamagnetic nanoparticles: synthesis, characterization, and performance in forward osmosis processes, Ind. Eng. Chem. Res., 50 (2011) 382–388.
[19] A. Zhou, H. Luo, Q. Wang, L. Chen, T.C. Zhang, T. Tao, Magnetic thermoresponsive ionic nanogels as novel draw agents in forward osmosis, RSC Adv., 5 (2015) 15359–15365.
[20] D. Zhao, S. Chen, P. Wang, Q. Zhao, X. Lu, A dendrimer-based forward osmosis draw solute for seawater desalination, Ind. Eng. Chem. Res., 53 (2014) 16170–16175.
[21] J. Wang, G. Meng, K. Tao, M. Feng, X. Zhao, Z. Li, H. Xu, D. Xia, J.R. Lu, Immobilization of lipases on alkyl silane modified magnetic nanoparticles: effect of alkyl chain length on enzyme activity, PLoS One, 7 (2012) e43478.
[22] E. Ranjbakhsh, A.K. Bordbar, M. Abbasi, A.R. Khosropour, E. Shams, Enhancement of stability and catalytic activity of immobilized lipase on silica-coated modified magnetite nanoparticles, Chem. Eng. J., 179 (2012) 272–276.
[23] L. Zhou, C. Gao, W. Xu, Robust Fe_3O_4/SiO_2-Pt/Au/Pd magnetic nanocatalysts with multifunctional hyperbranched polyglycerol amplifiers, Langmuir, 26 (2010) 11217–11225.
[24] X. Hu, L. Zhou, C. Gao, Hyperbranched polymers meet colloid nanocrystals: a promising avenue to multifunctional, robust nanohybrids, Colloid Polym. Sci., 289 (2011) 1299–1320.
[25] M. Darroudi, M. Hakimi, E. Goodarzi, R. Kazemi Oskuee, Superparamagnetic iron oxide nanoparticles (SPIONs): green preparation, characterization and their cytotoxicity effects, Ceram. Int., 40 (2014) 14641–14645.
[26] A. Razmjou, J. Mansouri, V. Chen, The effects of mechanical and chemical modification of TiO_2 nanoparticles on the surface chemistry, structure and fouling performance of PES ultrafiltration membranes, J. Membr. Sci., 378 (2011) 73–84.
[27] T.F. Tadros, Rheology of Dispersions: Principles and Applications, John Wiley & Sons, Germany, 2011.
[28] S.J. Fritz, Ideality of clay membranes in osmotic processes: a review, Clays Clay Miner., 34 (1986) 214–223.
[29] D. Li, X. Zhang, J. Yao, G.P. Simon, H. Wang, Stimuli-responsive polymer hydrogels as a new class of draw agent for forward osmosis desalination, Chem. Commun., 47 (2011) 1710–1712.
[30] N.T. Hancock, T.Y. Cath, Solute coupled diffusion in osmotically driven membrane processes, Environ. Sci. Technol., 43 (2009) 6769–6775.